

## RESEARCH ARTICLE

# Functional characterisation of the chromatically antagonistic photosensitive mechanism of erythrophores in the tilapia *Oreochromis niloticus*

Shyh-Chi Chen<sup>1,\*</sup>, Chengfeng Xiao<sup>1</sup>, Nikolaus F. Troje<sup>1,2,3</sup>, R. Meldrum Robertson<sup>1,3</sup> and Craig W. Hawryshyn<sup>1,3</sup>

**ABSTRACT**

Non-visual photoreceptors with diverse photopigments allow organisms to adapt to changing light conditions. Whereas visual photoreceptors are involved in image formation, non-visual photoreceptors mainly undertake various non-image-forming tasks. They form specialised photosensory systems that measure the quality and quantity of light and enable appropriate behavioural and physiological responses. Chromatophores are dermal non-visual photoreceptors directly exposed to light and they not only receive ambient photic input but also respond to it. These specialised photosensitive pigment cells enable animals to adjust body coloration to fit environments, and play an important role in mate choice, camouflage and ultraviolet (UV) protection. However, the signalling pathway underlying chromatophore photoresponses and the physiological importance of chromatophore colour change remain under-investigated. Here, we characterised the intrinsic photosensitive system of red chromatophores (erythrophores) in tilapia. Like some non-visual photoreceptors, tilapia erythrophores showed wavelength-dependent photoresponses in two spectral regions: aggregations of inner pigment granules under UV and short-wavelengths and dispersions under middle- and long-wavelengths. The action spectra curve suggested that two primary photopigments exert opposite effects on these light-driven processes: SWS1 (short-wavelength sensitive 1) for aggregations and RH2b (rhodopsin-like) for dispersions. Both western blot and immunohistochemistry showed SWS1 expression in integumentary tissues and erythrophores. The membrane potential of erythrophores depolarised under UV illumination, suggesting that changes in membrane potential are required for photoresponses. These results suggest that SWS1 and RH2b play key roles in mediating intrinsic erythrophore photoresponses in different spectral ranges and this chromatically dependent antagonistic photosensitive mechanism may provide an advantage to detect subtle environmental photic change.

**KEY WORDS:** Chromatophores, Opsins, Photoreceptors, Pigment cells, Visual pigments

**INTRODUCTION**

In mammals, eyes serve as the only photosensory organ to detect changes in the photic environment. In addition to eyes for vision, non-mammalian vertebrates and invertebrates possess multiple tissues and organs responsible for light reception (Vigh et al., 2002).

<sup>1</sup>Department of Biology, Queen's University, Kingston, Ontario, Canada K7L 3N6.

<sup>2</sup>Department of Psychology, Queen's University, Kingston, Ontario, Canada

K7L 3N6. <sup>3</sup>Centre for Neuroscience Studies, Queen's University, Kingston, Ontario, Canada K7L 3N6.

\*Author for correspondence at present address: Department of Ecology, Evolution and Behavior, The Alexander Silberman Institute of Life Sciences, The Hebrew University of Jerusalem, Jerusalem, 91904, Israel (shyhchi.chen@mail.huji.ac.il)

Received 17 April 2014; Accepted 18 December 2014

Non-visual photoreceptors are present in many locations on the body and play an important role in behaviour and physiological regulation. Of particular interest are the photosensitive mechanisms underlying diverse non-image-forming functions, such as circadian photoentrainment, the pupillary light reflex and skin pigmentation (Shand and Foster, 1999; Panda et al., 2002; Lucas et al., 2003). However, the mechanism of phototransduction and the response characterisation of many non-visual photoreceptors remain unclear.

Chromatophores are specialised dermal pigment cells that share a common embryological origin (the neural crest) with the retina. They are categorised as paraneurons and are known for their important roles in the regulation of body coloration (Fujii, 1993). To create body pattern or pigmentation, chromatophores can form 'chromatophore units' with other tissues or cells, change cell size or numbers, or adjust internal structures via movements of guanine plates or translocations of pigment granules (Fujii, 1969; Hawkes, 1974). In response to internal regulators (e.g. neurohormones) or external stimuli (e.g. light), chromatophores are able to make rapid, remarkable colour changes (Mäthger et al., 2003; Ban et al., 2005; Chen et al., 2013; Nilsson Sköld et al., 2013). For example, intrinsically photosensitive dermal chromatophores of the Nile tilapia *Oreochromis niloticus* demonstrate distinct photoresponses (Chen et al., 2013). Independent of wavelength, the black pigments (melanosomes) of melanophores tend to disperse and melanophores maintain dispersion state by shuffling pigment granules (Chen et al., 2013). By contrast, the aggregations and dispersion of red pigment (erythrosomes) of erythrophores are induced in different spectral ranges (Ban et al., 2005; Chen et al., 2013). Both visual and non-visual photopigments have been identified within isolated chromatophores and in tissues containing chromatophores (Provencio et al., 1998; Kasai and Oshima, 2006). Opsins are thought to initiate phototransduction by the regulation of intracellular cAMP level through G<sub>s</sub> and G<sub>i</sub> proteins, leading to pigment dispersion and aggregation, respectively (Ban et al., 2005). However, the downstream components of the signalling pathway have not been identified. Furthermore, how organisms coordinate different types of chromatophores to adjust body patterns and pigmentation under different photic environments remains unclear. Without detailed molecular evidence and functional characterisation, we do not know which molecules participate in the phototransduction of chromatophore photoresponses and how photopigments give rise to photoresponses in chromatophores.

In the present study, we aim to characterise tilapia erythrophore photoresponses and investigate the intrinsically photosensitive mechanism mediating photoreception. In the spectrum ranging from 380 to 600 nm, aggregation occurred in the UV/short-wavelength range whereas dispersion occurred with middle- and long-wavelengths. The action spectra further suggested that two primary opsins are responsible for distinct photoresponses. Using UV and middle-/long-wavelength chromatic adapting backgrounds, we

tested the hypothesis that erythrofore aggregations are mediated by SWS1 and dispersions by RH2b, two tilapia visual photopigments with maximal absorbances ( $\lambda_{\max}$ ) near the peaks in erythrofore action spectra (Spady et al., 2006). Using intracellular recording techniques, we found that the erythrofore photoresponses were associated with changes in membrane potential. Our findings suggest that tilapia cone photopigments are involved in erythrofore photoresponses and form a chromatically specific antagonistic photosensitive mechanism that is similar to those found in other non-visual photoreceptors like the reptile parietal eye and the amphibian frontal and pineal organs (Dodt and Heerd, 1962; Dodt and Morita, 1964; Dodt and Scherer, 1968).

## RESULTS

### Photic effects of chromatophores and chromatophore unit on tilapia integumentary tissues

In tilapia caudal fin, melanophores and erythrofores are the major classes of pigmented chromatophores contributing to colour pattern and pigmentation (Fig. 1A). Melanophores and erythrofores exert colour changes through aggregation and dispersion of their pigment granules (Fig. 1A,C,D). In addition, the formation of chromatophore units by different types of chromatophores generates diverse photic effects on body coloration. For example, under illumination at 380 nm, the dispersion of melanophores and the aggregation of erythrofores will lead to darker and less reddish body coloration (Fig. 1B).

### Action spectrum of erythrofores

Under illumination, erythrofores show photoresponses in a wavelength-dependent manner (Chen et al., 2013). To functionally characterise the action spectrum of erythrofore, we assessed the response of erythrofores to light ranging from 380

to 600 nm. Translocation of pigment granules took place in response to light stimuli of different wavelengths and the direction of erythrofore movement was dependent on the spectral range of stimulation: aggregations at 380–440 nm and dispersions at 460–600 nm (Fig. 2). Two peaks arising in the action spectrum of tilapia erythrofores suggested that one photopigment was responsible for aggregations and the other for dispersions (Fig. 2). The photosensitivity peaks present in the UV (380 nm) and middle-wavelength (480 nm) regions were close to the maximum absorbances ( $\lambda_{\max}$ ) of the tilapia retinal cone photopigments (SWS1, 360 nm; RH2b, 472 nm) (Spady et al., 2006). To better understand the interaction between photopigments, the visual pigment templates of SWS1 and RH2b were fitted to the erythrofore action spectrum plot (Govardovskii et al., 2000; Sabbah et al., 2012; Hornsby et al., 2013). Because of the opposing effects elicited by these two photopigments, a neutral area of the antagonistic interaction is suggested to be located in the spectral region near 440–460 nm, which is within the overlapping area of the  $\alpha$ -bands (the primary absorption peaks) of these two photopigments. Together, two photopigments may construct an intrinsic antagonistic mechanism responsible for light-driven erythrofore translocation.

### Effect of photopigment bleaching on erythrofore photoresponses

To investigate whether a chromatically-dependent antagonistic mechanism underlies tilapia erythrofore photoresponses, the effect of photopigment bleaching on photoresponses was assessed. Previous studies in visual systems have shown that chromatic adaptation selectively depresses photosensitivity of a particular photopigment and leaves the remaining cone mechanism with prominent sensitivity (Hawryshyn and Beauchamp, 1985;

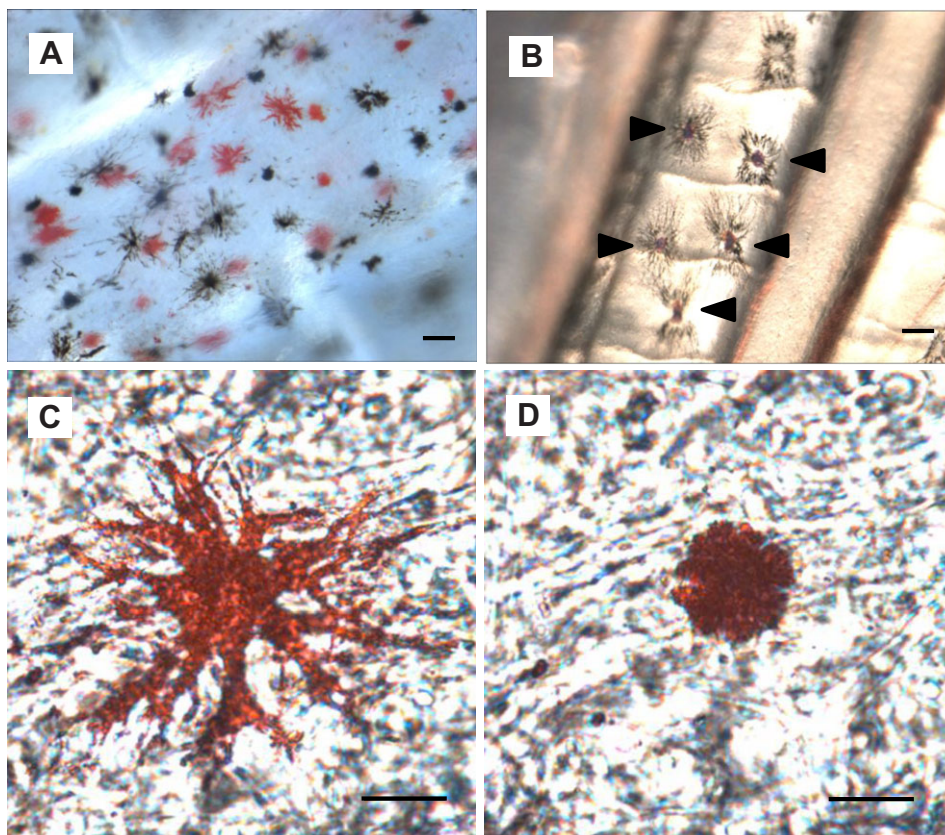


**Fig. 1. Chromatophore unit and erythrofore responses in the tilapia *Oreochromis niloticus*.** (A) Two major classes of pigmented chromatophores, black melanophores and red erythrofores, on split-fin tissue from the caudal fin. (B) Chromatophore units (arrowheads) consisted of aggregated erythrofores with dispersed melanophores. The arrangement of different types of chromatophores leads to dramatic photic effects due to the integration of motile activities of pigment cells. (C,D) An erythrofore dispersed (C) and aggregated (D) by means of the translocation of pigment granules. Scale bars: 80  $\mu\text{m}$  (A); 60  $\mu\text{m}$  (B); 20  $\mu\text{m}$  (C,D).

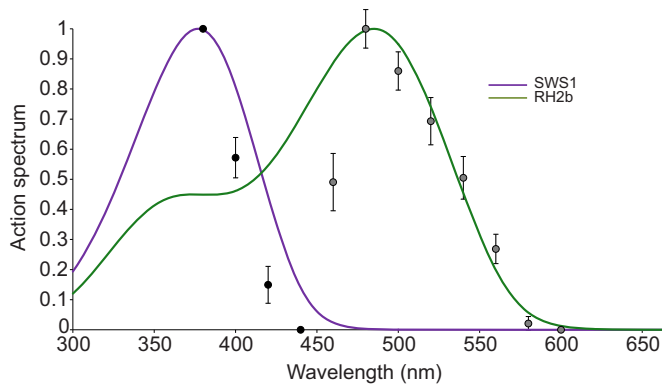


**Fig. 2. Functional characterisation of tilapia erythrofore photoreponses.** Tilapia erythrofores ( $N=17$ ) showed photoreponses in a wavelength-dependent manner. Aggregations occurred at UV and short wavelengths (380–440 nm; black circles) and dispersions at middle- and long-wavelengths (460–600 nm; grey circles). Two primary sensitivity peaks appeared at 380 and 480 nm, which are close to the absorption peaks of tilapia retinal photopigments with SWS1 (360 nm) and RH2b (472 nm) opsins (Spady et al., 2006). Erythrofore action spectrum was fitted with absorption templates of SWS1 (purple) and RH2b (green). The curve fitting showed that the antagonistic interaction between two opsins took place in the overlapping area of the absorption spectra of the alpha bands of SWS1 and RH2b (400–460 nm) (Govardovskii et al., 2000).

Hawryshyn, 1991; Lisney et al., 2010). Here, constant UV and yellow backgrounds were used to selectively depress two candidate photopigments sensitive to UV and middle wavelengths, SWS1 and RH2b, which were possibly responsible for erythrofore aggregations and dispersions, respectively. When UV chromatic adaptation was used, we found that compared with the control group without background light ( $N=5$ ), significant attenuation occurred in the extent of the aggregation (Tukey's test,  $P=0.002$ ;  $N=6$ ; Fig. 3A) but no significant change in dispersion ( $N=6$ ; Fig. 3A). With a bright yellow background, dispersion was reduced (Tukey's test,  $P<0.001$ ;  $N=7$ ; Fig. 3B) but, surprisingly, the degree of aggregation increased (Tukey's test,  $P=0.041$ ;  $N=8$ ; Fig. 3B). These results revealed that UV and yellow backgrounds caused the bleaching of SWS1 and RH2b. Furthermore, as a result of the antagonistic effect of the two photopigments, when RH2b was depressed the response elicited by SWS1 increased (Fig. 3B). However, under UV background, because of absorbance by the  $\beta$ -band of RH2b, RH2b might be also sensitive to UV light and get bleached to some degree. This could explain why we did not observe an increase in the amplitude of RH2b-driven dispersion when the strength of SWS1 was inhibited under UV background (Fig. 3A).

### Opsin protein expression in tilapia integumentary tissue and erythrofores

Following measurement of the action spectra of erythrofores in split-fin tissues, we used western blot analysis and immunohistochemistry to examine opsin expression in the tilapia caudal fin and individual erythrofores. Because an anti-RH2b antibody with low cross-reactivity to other opsin proteins is not available, in the present study we used anti-SWS1 antibody only. Using antibodies against SWS1, we detected the band at the expected size near 37 kDa (Fig. 4A). When immunohistochemistry was carried out in split-fin tissue containing erythrofores, an immunosignal was detected in individual erythrofores (Fig. 4B). A total of 16 cells from 3 fish were examined by immunostaining and all cells were found to express SWS1. These results are consistent with our findings in the opsin expression profile of

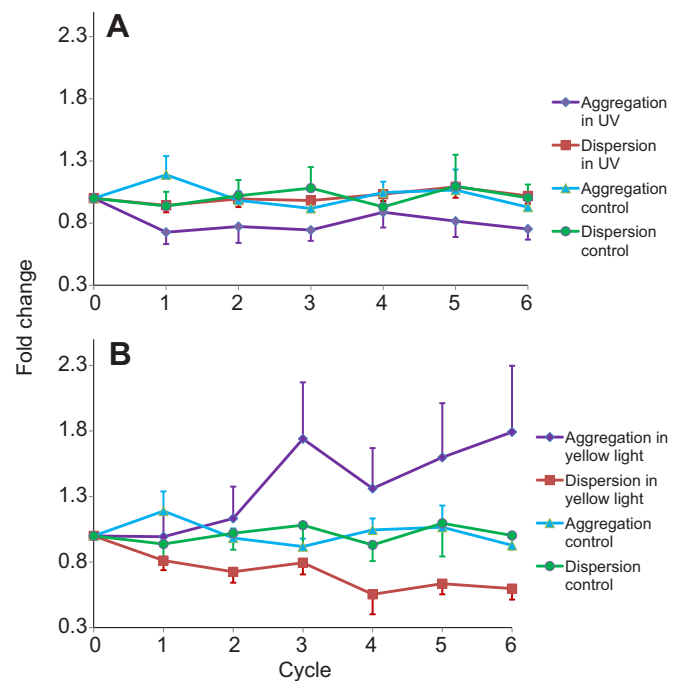


**Fig. 3. Effect of chromatic adaptation on erythrofore photoreponses.** (A,B) The fold change of aggregation at 380 nm and dispersion at 500 nm of erythrofores illuminated with UV (A) and yellow (B) backgrounds was compared with the photoreponses of the erythrofores without the treatment of background light (cycle 0). The control groups for aggregation and dispersion (blue and green lines) in A and B were made from the same data. Error bars show s.e.m.

erythrofores using single-cell RT-PCR (Chen et al., 2013) and together with the measurement of erythrofore action spectrum, strongly support the involvement of SWS1 in tilapia erythrofore photoreponses.

### Association between depolarisation and pigment aggregation under UV light in erythrofores

Non-visual photoreceptors with chromatic antagonism show distinct electrical characteristics (i.e. depolarisation and hyperpolarisation) in response to different wavelengths (Dodt and Meissl, 1982; Solessio and Engbretson, 1993; Shand and Foster, 1999). In tilapia erythrofores, SWS1 and RH2b may initiate two major photosensing cascades that eventually lead to the opening of selective cation channels in the membrane and the changes of membrane potential. Unlike the light-activated instant phototransduction and hyperpolarisation of photoreceptors in the retina, the SWS1-expressing erythrofores perhaps undergo depolarisation. For example, it is the depolarisation that was closely associated with the pigment aggregation in squirrelfish *Holocentrus* erythrofores (Luby-Phelps and Porter, 1982). To test whether SWS1 or RH2b in erythrofores are differentially involved in the membrane potential change, we examined the erythrofore membrane potential using broad-spectrum UV or yellow light. An abrupt shift in the recorded potential (from 0 mV to about  $-30$  mV) indicated the successful penetration of an electrode into an erythrofore and the measurement of a membrane potential (Fig. 5A). UV illumination on dark-adapted erythrofores induced a gradual depolarisation of membrane potential reaching a plateau after 3–5 min. This time scale precisely coincided with the pigment aggregation with observed UV illumination (Chen et al., 2013). The depolarisation amplitude was around 20 mV, and turning off the illumination did not restore the membrane potential within 10 min

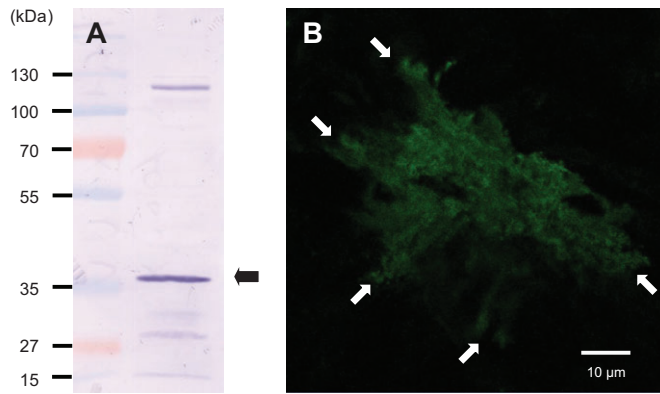


**Fig. 4. Western blot analysis and immunohistochemistry of SWS1 opsin in tilapia integumentary tissue and erythrophore.** (A) Proteins extracted from caudal fins were subjected to western blot analysis. Blots were probed with the antibody against SWS1. After incubation with NBT/BCIP, SWS1 opsin was detected at its expected size (37 kDa; arrow). (B) Immunohistochemistry of SWS1 expression was detected within erythrophores. The dendritic processes of the erythrophore are indicated by arrows.

(Fig. 5Bi,ii,  $N=3$ ). We also observed that the aggregation status persisted for more than 10 min in the dark. Perhaps a period longer than 10 min is required for the restoration of membrane potential after a plateau of depolarisation sustained for several minutes. Interestingly, depolarisation was not observed in erythrophores, which did not respond to UV illumination and showed no pigment aggregation (Fig. 5Biii). There was also no depolarisation in unstimulated erythrophores (Fig. 5Biv). Membrane potential changes in response to broad-spectrum yellow light were also examined. We did not detect changes in membrane potential under yellow light (Fig. 5Ci;  $N=18$  from 6 fish) although we observed the dispersion of erythrophores after light exposure. To ensure the responsiveness of erythrophores, we dark-adapted an aggregated erythrophore for 20 min and applied yellow light for 10 min. Again, the expected hyperpolarisation in the erythrophore was not seen (Fig. 5Cii). Although it is still questionable whether tilapia erythrophores are capable of demonstrating two opposing electrical responses similar to other non-visual photoreceptors, these data indicate the strong association between depolarisation and pigment aggregation under UV light in erythrophores.

## DISCUSSION

Our knowledge of how non-mammalian vertebrates sense ambient photic environments has been greatly advanced by investigating a variety of photosensitive tissues and novel opsins. Notably, studies on the pineal complex and deep brain have enhanced our understanding of non-image-forming visual tasks in non-visual photoreceptors (Meissl and Ekström, 1988; Uchida and Morita, 1994; Kojima et al., 2000; Nakane et al., 2010). However, because of the complexity of non-visual photoreceptors with varying photopigment repertoires, little is known about how photoreception and activation of the phototransduction cascade take place within such photosensitive organs or cells.

In the present study, we demonstrated that tilapia erythrophores respond to light in a wavelength-dependent manner. In the action spectrum curve, two response peaks were present in UV and middle-wavelength regions. We suggest that two primary photopigments are involved in the chromatic antagonism of erythrophores and are responsible for distinct photoresponses, i.e. SWS1 for aggregation and RH2b for dispersion. Indeed, western blot and immunohistochemistry revealed SWS1 expression although RH2b was not tested. Using the technique of chromatic adaptation, the degree of SWS1-associated

aggregation was attenuated under a constant UV background and the extent of RH2b-associated dispersion diminished under a yellow background. In addition, intracellular recording revealed that depolarisation occurred when cells were illuminated with UV light, suggesting erythrophore membrane potential changes along with light-induced responses. In spite of a neutral area at 440–460 nm suggested in the present study (Fig. 6), we expect that the neutral point is closer to the UV region based on the spectral absorbances of SWS1 and RH2b. The template fitting of the erythrophore action spectrum revealed that the peaks were narrower in the long-wavelength limb of SWS1 and the short-wavelength limb of RH2b. The template fit less well in the latter region, indicating a greater inhibitory effect on this region of RH2b and thus perhaps explaining why the neutral area moved toward middle-wavelength region. In addition to RH2b, other photopigments sensitive to middle-wavelengths may contribute to erythrophore photoresponses. For example, *RH2aβ* was expressed in 43% of tilapia erythrophores (Chen et al., 2013). However, these opsins combined with the A1 or A2 type chromatophore do not render peak absorbances as close to 480 nm as RH2b, suggesting that the photopigment with RH2b is more likely to be the primary photopigment responsible for dispersion. Given the importance of RH2b, the expression of RH2b should be high in erythrophores. The previous study showed lower expression of RH2b compared with that of other opsins (Chen et al., 2013). This could be because the RT-PCR was conducted in integumentary tissues containing other types of chromatophores. It is also worth mentioning that some erythrophores were insensitive to yellow light, which could be due to no RH2b expression in these erythrophores. Chen et al. (2013) showed that single-cell RT-PCR analysis detected *RH2b* expression only in 57% of the erythrophores, suggesting that without RH2b expression, some erythrophores no longer respond to middle wavelengths. However, in this study, we found UV-sensitive and -insensitive erythrophores when measuring the membrane potential change under UV illumination (Fig. 5B). Because these cells had no morphological difference, it remains unclear whether these UV-insensitive erythrophores are immature cells or belong to a subclass of erythrophores. More experiments such as *in situ* hybridization or RT-PCR at the single-cell level should be carried out to answer these questions.

In teleosts and reptiles, chromatophores on the dermal layer are the primary agents for the generation of extraordinary body patterns. In addition to neural and hormonal regulation, chromatophores can respond directly to light and thus they are categorised as non-visual photoreceptors. Their ability to respond to incident light varies in a species-specific manner and also depends on developmental stage (Naora et al., 1988; Moriya et al., 1996; Oshima et al., 1998; Chen et al., 2014). Like other photoreceptors, chromatophore photosensitivity is proposed to be associated with the expression of opsin-based photopigments within cells (Ban et al., 2005). Using molecular approaches, opsin expression has been identified in tissues containing chromatophores and in pigment cell lines (Miyashita et al., 2001; Kasai and Oshima, 2006; Im et al., 2007). However, some of these results have been obtained from tissues that may contain a mixture of different types of chromatophores. In addition, it is not a guarantee that an expressed opsin is functional for photoresponses (Shand and Foster, 1999). The direct correlation between chromatophore photoresponses and opsin expression remains poorly understood and more functional characterisation of photoresponses is required to clarify the involvement of opsins in photosensitive processes. Recently, using single-cell RT-PCR, co-expression of different types of cone opsin genes was found in Nile tilapia erythrophores, which respond to light in a wavelength-

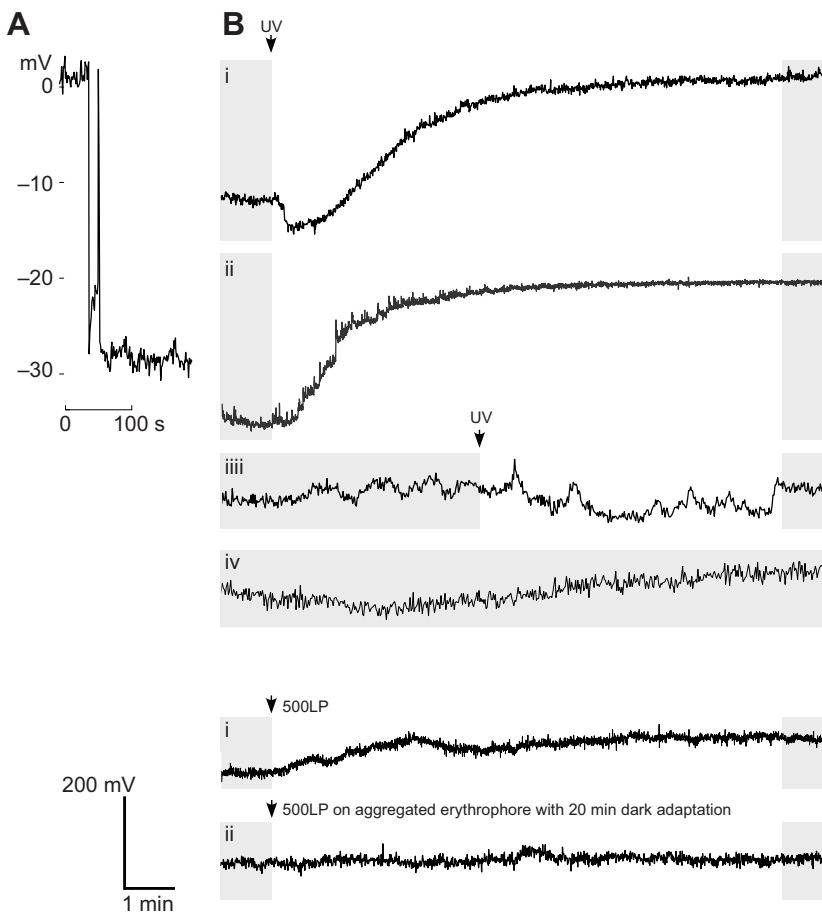


**Fig. 5. Change in membrane potential of erythroophores under illumination.**

(A) Representative trace showing an abrupt membrane potential shift from 0 to  $-30$  mV when the electrode successfully penetrated the cell membrane. (B) Under UV illumination, depolarisation took place with aggregation of two erythroophores (i,ii). (iii) A recording from an erythroophore insensitive to UV. (iv) A recording from an erythroophore in the dark. (C) There is no apparent change of membrane potential of the erythroophore upon illumination with yellow light (500LP) (i) or on an aggregated erythroophore upon illumination with yellow light (500LP) after 20 min dark adaptation (ii). The grey area in each panel indicates the period of darkness.

dependent manner (Chen et al., 2013). The expression profile of erythroophores implied that genes in the *sws1* and *rh2* groups (specifically *rh2b*, *rh2a $\beta$*  and *rh2a $\alpha$* ) are prime candidates to play important photosensitive roles (Chen et al., 2013). A similar co-expression repertoire of UV (*sws1*) and green (*rh2*) photopigments and its physiological importance were identified in another type of non-visual organ, the pineal gland of the Atlantic halibut *Hippoglossus hippoglossus* (Forsell et al., 2001, 2002). The peaks at UV and middle-wavelength areas in the action spectrum for erythroophores indicated that the chromatic antagonism in tilapia erythroophores is similar to other non-visual photoreceptors (Uchida and Morita, 1990; Solessio and Engbretson, 1993).

Non-visual photoreceptors are considered to serve as photon flux detectors and are involved in many non-image-forming sensory tasks, such as circadian photoentrainment, body coloration and behaviour orientation (Hayashi et al., 1993; Meissl and Yanez, 1994; Binder and McDonald, 2008). Among these, the studies on parietal eyes, deep brain and pineal photoreceptors have provided comparative information about the response characteristics of some non-visual photoreceptors. Recordings from these photosensitive tissues/organs show two types of electrical response under illumination. One type is achromatic (not colour coded), and is involved in the inhibitory action of light regardless of wavelengths (Hartwig and Baumann, 1974; Meissl and Ueck, 1980; Meissl and Ekström, 1988). The other shows a chromatic response where an inhibitory component is sensitive to short wavelengths and an excitatory component is sensitive to middle/long wavelengths (Dodt and Heerd, 1962; Uchida and Morita, 1990; Solessio and Engbretson, 1993). For example, the parietal (third) eye of lizards displays chromatically dependent responses consisting of

short-wavelength-sensitive hyperpolarisation and green-sensitive depolarisation (Solessio and Engbretson, 1993). This chromatically dependent antagonistic mechanism in the lizard parietal eye photoreceptors is composed of two non-visual photopigments, UV-sensitive parapinopsin and green-sensitive parietopsin, and is suggested to assess cyclic spectral variation and enhance twilight detection (Shand and Foster, 1999; Wada et al., 2012). Tilapia light-sensitive erythroophores may also use a colour-opponent system for wavelength discrimination. Interestingly, contrary to other types of non-visual photoreceptors, intracellular recording from tilapia erythroophores reveals that depolarisation (excitatory component) was associated with UV-driven aggregation. Taken together, we suggest that reversing the electrical signals may enable tilapia erythroophores to enhance spectral discrimination and detect subtle photic changes in environmental light conditions through measuring the ratio change of different wavelengths. In addition, because the middle/long-wavelength-induced dispersion will lead to the body color shifting toward the red, tilapia may benefit from this color change, which makes it more cryptic in the middle/long-wavelength-rich background. Two photopigments, SWS1 and RH2b, contribute to ‘chromatic’ erythroophore photoresponses in different spectral regions, instead of an ‘achromatic’ response. Therefore, this spectral discrimination, together with the photic effects caused by aggregation and dispersion, will be advantageous for tilapia to fit its surrounding environments.

Emerging novel opsins have been reported in various types of photoreceptors. In teleosts, the sequences, localisations and expression patterns of some non-visual photopigments have been investigated. For example, melanopsin occurs in cod skin (Drivenes et al., 2003), VA opsin in the pineal organ of Atlantic salmon (Philp

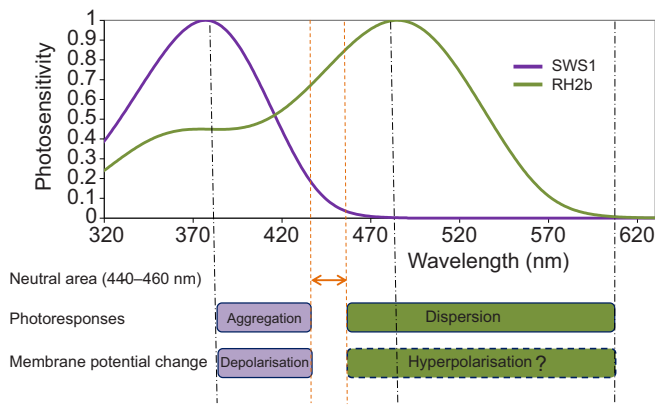


**Fig. 6. Model for the chromatically dependent antagonistic mechanism of tilapia erythrofore photoreponses.** A schematic diagram showing that SWS1 and RH2b have antagonistic effects on erythrofore photoreponses. SWS1 is responsible for aggregations in UV and short-wavelength regions and RH2b for dispersions in middle and long wavelengths. The antagonistic interaction between SWS1 and RH2b occurs in the overlapping area of the absorption curves of these two opsins. The orange double-sided arrow indicates the possible region where the neutral point of this interaction is located. Erythrofore photoreponses are associated with the membrane potential changes because depolarisation takes place with aggregation. The occurrence of the proposed hyperpolarisation during dispersions was not observed in the present study (dashed rectangle).

et al., 2000), parapinopsin in the parapineal organ of catfish (Blackshaw and Snyder, 1997) and exo-rhodopsin in the zebrafish pineal gland (Mano et al., 1999). In tilapia, neither non-visual opsins [melanopsin (*opn4*) and teleost multiple tissue (*tmt*) opsin] nor rod opsin [rhodopsin (*rh1*)] have been detected in individual erythrofores or integumentary tissues (Chen et al., 2013). More likely, therefore, is that erythrofore phototransduction may be initiated by cone opsin-based photopigments, i.e. SWS1 and RH2b. Interestingly, since the expression level of *sws1* and *rh2b* in tilapia retinal photoreceptors is very low (Spady et al., 2006), our results demonstrate that this non-visual photosensory systems in tilapia erythrofores uses a different opsin repertoire for non-visual photoreception. Because of the diversity of opsins, however, we cannot completely rule out the possibility that other types of non-visual opsins are involved in this photosensitive process. Increasing evidence has shown that some photopigments are bistable and possess absorption maxima in two spectral regions, for example, chicken neuropsin (cOpn5m) with  $\lambda_{\max}$  at 360 and 474 nm, and lamprey parapinopsin with  $\lambda_{\max}$  at 370 and 515 nm (Koyanagi et al., 2004; Yamashita et al., 2010). Thus, these bistable photopigments alone may be sufficient to induce photoreponses in two spectral regions through different signalling pathways. In the future, thorough investigation of the photopigment expression profile of erythrofores and their contributions to erythrofore photoreponses should be undertaken, particularly in those whose  $\lambda_{\max}$  are close to the peaks of erythrofore action spectrum (e.g. cryptochrome and VA opsin).

In conclusion, much research has focused on non-visual photoreception and the relevant sensory tasks of non-visual photoreceptors. In the present study, we investigated the action spectrum of erythrofores and the chromatically dependent antagonistic mechanisms that underlie erythrofore photoreponses (Fig. 6). Collectively, our data suggest that SWS1 and RH2b activation leads to aggregation under UV/short-wavelength

illumination and dispersion with middle/long-wavelength light. In addition, depolarisation was detected when aggregation was induced by UV light. Tilapia may benefit from these response characteristics so that they can systematically detect changes in environmental light. To date, the tilapia erythrofore and rainbow trout melanophore (Chen et al., 2014) are the only two types of chromatophores showing chromatically antagonistic photoreponses. They offer a great opportunity to study colour-opponent systems because, compared with other types of photoreceptors, it is easy to identify these cells because of their red and black pigments and it is feasible to isolate and culture chromatophores for further treatments, such as immunosuppression using antibodies against opsins (Ban et al., 2005; Oshima et al., 1996). Our findings demonstrate that tilapia erythrofores offer an excellent and accessible model for studying colour-opponent systems and interaction between photopigments that may overcome the functional limitations experienced with other types of photoreceptors.

## MATERIALS AND METHODS

### Animals

Adult male Nile tilapia *Oreochromis niloticus* Linnaeus 1758 were obtained from a local fish farm, Northern American Tilapia Inc. (Lindsay, ON, Canada). Fish with average standard lengths ( $14.7 \pm 0.8$  cm) and weight ( $48.5 \pm 6.0$  g) were used in this study. Fish were maintained at a water temperature of 25°C under a 12 h:12 h light:dark cycle. Light was provided by full spectrum fluorescent lamps. Since circadian influences on opsin expression and pigmentary patterns have been reported in fish, dissections were always carried out from 11:00 to 13:00 (Masagaki and Fujii, 1999; Johnson et al., 2013). Studies on cichlids showed the rhythmicity of opsin expression in the retina (Korenbrod and Fernald, 1989; Halstenberg et al., 2005) and currently no relevant observation has been reported in tilapia retinal photoreceptors or other photoreceptor types. In order to avoid any possible influence on our measurements due to the opsin expression variation and to maintain consistency, we sampled the fish during this specific time window. Fish were dark adapted for 30 min and anaesthetised with MS-222 before use (Crescent Research Chemical, Phoenix, AZ, USA). All procedures complied with the Canadian Council for Animal Care regulations and the Queen's University Animal Care Committee.

### Preparation of split-fin tissues

Split-fin tissues were prepared by methods described previously (Masada et al., 1990; Fujii et al., 1991). Excised tilapia caudal fins were rinsed with 70% ethanol and  $\text{Ca}^{2+}$ ,  $\text{Mg}^{2+}$ -free, Dulbecco's phosphate-buffered saline (CMF-PBS: 136.9 mmol  $\text{l}^{-1}$  NaCl, 2.7 mmol  $\text{l}^{-1}$  KCl, 8.1 mmol  $\text{l}^{-1}$   $\text{Na}_2\text{HPO}_4$ , 1.5 mmol  $\text{l}^{-1}$   $\text{KH}_2\text{PO}_4$ , pH 7.2). After being cut into 5 mm<sup>2</sup> pieces, fin tissues were incubated in EDTA-bicarbonate solution (pH 7.4) for 20 min, followed by vigorous shaking in 0.25% collagenase type II (Sigma-Aldrich, St Louis, MO, USA) for 30 min. Split-fin tissues containing chromatophores were incubated in culture medium (mixture of Leibovitz L15 medium, fetal calf serum, and water in a ratio 80:15:5, 100 U  $\text{ml}^{-1}$  penicillin-G, 100  $\mu\text{g ml}^{-1}$  kanamycin) at 25°C in a water-jacketed  $\text{CO}_2$  incubator in the dark for 2 days. After 2 days of culture, tissues were immersed in PBS (125.3 mmol  $\text{l}^{-1}$  NaCl, 2.7 mmol  $\text{l}^{-1}$  KCl, 1.8 mmol  $\text{l}^{-1}$   $\text{CaCl}_2$ , 1.8 mmol  $\text{l}^{-1}$   $\text{MgCl}_2$ , 5.6 mmol  $\text{l}^{-1}$  D-glucose, 5.0 mmol  $\text{l}^{-1}$  Tris-HCl buffer, pH 7.2) for 15 min dark adaptation before experiments.

### Measurements of erythrofore photoreponses

Light stimuli were generated by a 150 W xenon lamp system and a monochromator (Photon Technology International, London, ON, Canada). A background channel with 250 W quartz-halogen lamps (Ushio, Cypress, CA, USA) was used for taking images. As it has been suggested that aggregations occur near UV and dispersions at 500 nm (Sato et al., 2004), light at 380 nm ( $12.89 \log \text{photons cm}^{-2} \text{ s}^{-1}$ ) and 500 nm ( $13.21 \log \text{photons cm}^{-2} \text{ s}^{-1}$ ) was used to induce full aggregations or dispersions at the

beginning of each measurement. Adequate time (not reaching saturation, i.e. full aggregation or dispersion) to assess photoresponses was determined by means of measuring the time course of aggregation under 380 nm light (12.89 log photons  $\text{cm}^{-2} \text{s}^{-1}$ ) and dispersion under 500 nm light (13.21 log photons  $\text{cm}^{-2} \text{s}^{-1}$ ). For measuring aggregation at 380 nm, cells were stimulated with light at 500 nm for 3 min, and kept in the dark for 3 min to obtain full dispersion. Subsequently, a light stimulus at 380 nm was applied to elicit aggregation. Similarly, for dispersion at 500 nm, cells were stimulated with light at 380 nm for 3 min, and kept in the dark for 3 min to obtain full aggregation. Then, a light stimulus at 500 nm was applied to induce dispersion. The duration  $t$  for illumination varied from 0 to 300 s for aggregation at 380 nm and from 0 to 800 s for dispersion at 500 nm in 20 s increments.

The cell responses to these light stimuli were measured in terms of the area covered by the red pigment which characterises the erythrocyte. It is known that the redness of erythrocytes is due to the erythrocytes being coloured with carotenoids (Fujii, 1993). For the analysis, we used a Nikon Eclipse E600FN microscope (Nikon, Mississauga, ON, Canada) with a Qimaging Microimager II CCD camera and QCapture Suite V2.46 software (Qimaging, Burnaby, BC, Canada). First, a selection tool with a rectangular region of interest (ROI) was applied to a single erythrocyte to cover the cell dendrites as tightly as possible. Then, automated image analysis was performed in MATLAB (MathWorks, Natick, MA, USA) counting the pixels that represent the pigmented area of erythrocytes. Red pixels were automatically identified as every pixel in which the values for the red channel were larger than both the values of the green and blue channels in RGB colour space. The total number of extracted red pixels represented the pigment-covered area. The maximum capacity ( $A_0$ ) for the translocation of pigment granules was calculated as:

$$A_0 = A_{\text{full dispersion}} - A_{\text{full aggregation}} \quad (1)$$

where  $A_{\text{full dispersion}}$  and  $A_{\text{full aggregation}}$  denote the pigmented area of each cell at full dispersion and aggregation status, respectively. The magnitude of the photoresponses was assessed through measuring the change of the pigmented area ( $A$ ) with  $A_t$  being the pigmented area at time  $t$  after stimulation onset. For dispersion, we determined the time required to reach half-maximal photoresponse as the time  $t$  for which  $A/A_0 = (A_t - A_{\text{full aggregation}}) / (A_{\text{full dispersion}} - A_{\text{full aggregation}}) = 0.5$ . Similarly, for aggregation we measured the time at which  $A/A_0 = (A_t - A_{\text{full dispersion}}) / (A_{\text{full dispersion}} - A_{\text{full aggregation}}) = 0.5$ . (aggregation: 61 s; dispersion: 194 s; supplementary material Fig. S1).

To avoid chromatic adaptation, erythrocyte photoresponses were measured in 20 nm increments from 380 to 600 nm with a staggered wavelength presentation (e.g. the order of stimulating wavelengths used for dispersion: 600, 520, 580, 500, 560, 480, 540 and 460 nm; for aggregation: 440, 380, 420 and 400 nm). No difference was found in the spectral sensitivity curve when light stimulation was conducted in the opposite order. At the beginning of each measurement, complete aggregation or dispersion was obtained through the illumination at 380 nm or 500 nm for 3 min, followed by 3 min of darkness. Subsequently, a light stimulus (380–440 nm: 12.89 log photons  $\text{cm}^{-2} \text{s}^{-1}$ , 61 s; 460–600 nm: 13.21 log photons  $\text{cm}^{-2} \text{s}^{-1}$ , 194 s) with 10 nm FWHM values (full width at half maximum) was applied to cells and then the spectral sensitivity ( $S_\lambda$ ) was determined as the erythrocyte photoresponse at each test wavelength ( $\lambda$ ) via measuring the change of the pigmented area using the aforementioned method for aggregation:

$$S_\lambda = |A_\lambda - A_{\text{full dispersion}}| / A_0 \quad (2)$$

and for dispersion:

$$S_\lambda = |A_\lambda - A_{\text{full aggregation}}| / A_0, \quad (3)$$

where  $A_\lambda$  denotes the pigmented area of each cell at assigned test wavelength  $\lambda$ . To create the spectral sensitivity curve, the spectral sensitivity was plotted against the test wavelengths. All the experiments were conducted at 25°C in darkness and tissues were continuously perfused with PBS.

## Curve fitting

In order to better interpret the interaction between opsins, absorption templates of putative opsins were used to fit the erythrocyte spectral sensitivity curve. The tilapia retina possesses seven cone opsins forming distinct visual pigments which have been proved functional (Spady et al., 2006; Carleton et al., 2008). The spectral characteristics of each pigment have been well-established from absorbance spectra of *in vitro* reconstituted proteins and from *in situ* microspectrophotometry (MSP) measurement (Spady et al., 2006; Carleton et al., 2008; Lisney et al., 2010). Based on reported sensitivity peaks of tilapia cone pigments (Spady et al., 2006), absorption templates were used to fit the photosensitivity curve using a least-squares fit as described previously (Govardovskii et al., 2000; Anderson et al., 2010; Hornsby et al., 2013). In the action spectrum curve of tilapia erythrocytes, two peaks present at 380 and 480 nm were close to the maximum absorbances ( $\lambda_{\text{max}}$ ) of the retinal cone photopigments (SWS1, 360 nm; RH2b, 472 nm; with 11-*cis*-retinal; Spady et al., 2006). Therefore, the templates for tilapia SWS1 and RH2b were used in the present study. The absorption spectra of the visual pigments depend not only on the opsin they use, but also the relative amounts of A1 (retinaldehyde) and A2 (3,4-didehydroretinaldehyde) chromophore they are containing (Leow, 1995). We estimated this relative amount by fitting the data obtained from the aggregation experiments with a linear combination of the templates for the spectral sensitivity ( $S$ ) of SWS1 obtained from pigments containing only A1 or only A2:

$$S_{\text{SWS1}}(\alpha) = \alpha \times S_{\text{SWS1,A2}} + (1 - \alpha) \times S_{\text{SWS1,A1}} \quad (4)$$

Likewise, we considered changes in absorption due to chromophore composition in RH2b:

$$S_{\text{RH2b}}(\alpha) = \alpha \times S_{\text{RH2b,A2}} + (1 - \alpha) \times S_{\text{RH2b,A1}}, \quad (5)$$

where the range of  $\alpha$  is  $0 \leq \alpha \leq 1$  (Hornsby et al., 2013). In freshwater fish species, A2 chromophore is favoured in retinal photoreceptors (Carleton et al., 2008). Since the exact A2 proportion in tilapia erythrocytes is unknown and SWS1 is the most likely photopigment responsible for the peak at 380 nm in the spectral sensitivity curve,  $\alpha$  is determined by fitting SWS1 template and subsequently applied to RH2b template.

## Photoresponse measurement under chromatic adapting background light conditions

Chromatic adaptation is a technique used to isolate a specific photoreceptor mechanism dominant at a particular spectral region (Hawryshyn, 1991; Hawryshyn et al., 2010; Sabbah et al., 2010). Since SWS1 and RH2b are suggested to be responsible for erythrocyte aggregations at UV/short-wavelength range and dispersions in middle/long wavelengths, two chromatic adapting background light conditions [a broad-spectrum yellow background by a long-wavelength pass interference filter with a cut-off wavelength of 500 nm (500LP) and a broad-spectrum UV background with a band-pass filter that peaked at 377 nm interference and neutral density (1.0 ND) filters; Corion, Franklin, MA, USA; supplementary material Fig. S2] were used to bleach photopigments most sensitive to these two spectral regions. To assess the effect of adaptation on photoresponses, we measured erythrocyte aggregations at 380 nm and dispersion at 500 nm under constant background light using the aforementioned method for measuring erythrocyte photoresponses for six cycles. At the beginning of each cycle, full aggregations or dispersions were induced by 3 min light exposure at 380 or 500 nm. Following a 3 min interstimulus interval with no stimulation (the background was kept constantly on throughout the measurements), a light stimulus at 500 or 380 nm was applied to induce erythrocyte photoresponses (supplementary material Fig. S3). Similarly, between each measuring cycle, a 3 min interstimulus interval without stimulation was applied and background light was kept on. The fold change of responses under adaptation was evaluated by comparison to the photoresponses obtained before background light was turned on. Photoresponses measured without background light were used as a control.

## Western blot

Western blots were performed using rat anti-rainbow trout UV opsin (homologue of tilapia SWS1; refer to Allison et al., 2006). Proteins were extracted from tilapia caudal fins through homogenisation in ice-cold cell lysis buffer (50 mmol l<sup>-1</sup> Tris-HCl, pH 8.0, 150 mmol l<sup>-1</sup> NaCl, 1% Triton X-100). Subsequently, lysates were centrifuged at 12,000 r.p.m. for 10 min at 4°C. Supernatants were collected and used in western blot with the aforementioned antisera. Proteins were resolved in a 10% SDS-polyacrylamide gel and transferred to a PVDF membrane. After being blocked with blocking solution [5% non-fat dry milk in PBST (PBS with 0.1% Tween20)] for 2 h at room temperature, membranes were incubated with antibodies (anti-UV, 1:1000, diluted in blocking solution) at 4°C overnight. Following several washes with PBST, immunosignals were further detected by goat anti-rat IgG antibody conjugated to alkaline phosphatase (Vector Laboratories, Burlingame, CA, USA) and visualised with BCIP/NBT (5-bromo-4-chloro-3-indolylphosphate/nitro-blue tetrazolium; Calbiochem, San Diego, CA, USA).

## Whole-mount immunohistochemistry

Split-fin tissues were fixed in 4% paraformaldehyde in phosphate-buffered solution (PBS, pH 7.4) at 4°C overnight. Subsequently, fixed skin tissues were blocked with 5% normal goat serum and 0.3% Triton X-100 in PBS for 1 h at room temperature. After several washes with PBS, tissues were incubated with antibodies against SWS1 (anti-UV, 1:1000, diluted in blocking solution) at 4°C overnight. Following the primary antibody incubation, immunoreactions were detected with Alexa-Fluor-488-conjugated goat anti-rat antibodies (Vector Laboratories, Burlingame, CA, USA) in the blocking buffer (10% normal goat serum and 0.1% sodium azide in PBS).

## Intracellular recording

Intracellular recordings were taken from erythrophores on tilapia scales, which were in PBS in the darkness for 15 min before measurements. The electrodes were prepared using aluminosilicate glass capillaries (SM100F-7.5; Harvard Apparatus LTD, Edenbridge, Kent, UK) and a Flaming/Brown Micropipette Puller (Model P-97; Sutter Instrument CO, CA, USA). The tip diameter of the electrodes was approximately 1 µm and the resistance was approximately 60 MΩ. The electrodes were filled with 1 mol l<sup>-1</sup> KCl and electrical signals were recorded by a Micro 1401 II interface and Signal data acquisition system (CED, Cambridge, UK). Illumination was provided by X-Cite 120 illuminator (EXFO Photonic Solutions, Mississauga, ON, Canada) with aforementioned interference filters and neutral density (ND) filter (2.0 ND; Corion, Franklin, MA, USA).

## Statistical analysis

The photoresponses of the groups illuminated with light adaptation were compared with the photoresponses of the groups without background light. The data were analyzed by a two-way ANOVA using SigmaPlot statistical software 11.0 (Systat Software Inc., Point Richmond, CA, USA), followed by Tukey's HSD test used for *post hoc* analysis of the significant effects ( $P < 0.05$ ).

## Acknowledgements

We would like to thank Manisha Bhardwaj, Zahra Dargaei, and Stephanie Zahradnik for their assistance with data collection. We thank Dr Dongshen Tu, Dr Shai Sabbah, Dr Jun Liu, Dr Thomas Kuiran Chen, Dr Shan Jiang, Dr Yi Niu, Mark Hornsby and Zhen Wang for their helpful discussions and insights.

## Competing interests

The authors declare no competing or financial interests.

## Author contributions

Conceived and designed the experiments: S.C.C. and C.W.H. Performed the experiments: S.C.C. Analyzed the data: S.C.C., C.X. and N.F.T. Contributed reagents/materials/analysis tools: C.W.H. Wrote the paper: S.C.C. Critically read the manuscript: N.F.T., R.M.R. and C.W.H.

## Funding

This study was supported by an NSERC Discovery Grant, the Canada Research Chairs program, Canada Foundation for Innovation (to C.W.H.).

## Supplementary material

Supplementary material available online at <http://jeb.biologists.org/lookup/suppl/doi:10.1242/jeb.106831/-DC1>

## References

- Allison, W. T., Dann, S. G., Veldhoen, K. M. and Hawryshyn, C. W. (2006). Degeneration and regeneration of ultraviolet cone photoreceptors during development in rainbow trout. *J. Comp. Neurol.* **499**, 702–715.
- Anderson, L. G., Sabbah, S. and Hawryshyn, C. W. (2010). Spectral sensitivity of single cones in rainbow trout (*Oncorhynchus mykiss*): a whole-cell voltage clamp study. *Vision Res.* **50**, 2055–2061.
- Ban, E., Kasai, A., Sato, M., Yokozeki, A., Hisatomi, O. and Oshima, N. (2005). The signaling pathway in photoresponses that may be mediated by visual pigments in erythrophores of Nile tilapia. *Pigment Cell Res.* **18**, 360–369.
- Binder, T. R. and McDonald, D. G. (2008). The role of dermal photoreceptors during the sea lamprey (*Petromyzon marinus*) spawning migration. *J. Comp. Physiol. A Neuroethol. Sens. Neural. Behav. Physiol.* **194**, 921–928.
- Blackshaw, S. and Snyder, S. H. (1997). Parapinopsin, a novel catfish opsin localized to the parapineal organ, defines a new gene family. *J. Neurosci.* **17**, 8083–8092.
- Carleton, K. L., Spady, T. C., Streelman, J. T., Kidd, M. R., McFarland, W. N. and Loew, E. R. (2008). Visual sensitivities tuned by heterochronic shifts in opsin gene expression. *BMC Biol.* **6**, 22.
- Chen, S.-C., Robertson, R. M. and Hawryshyn, C. W. (2013). Possible involvement of cone opsins in distinct photoresponses of intrinsically photosensitive dermal chromatophores in tilapia *Oreochromis niloticus*. *PLoS ONE* **8**, e70342.
- Chen, S.-C., Robertson, R. M. and Hawryshyn, C. W. (2014). Ontogeny of melanophore photosensitivity in rainbow trout (*Oncorhynchus mykiss*). *Biol. Open* **3**, 1032–1036.
- Doty, E. and Heerd, E. (1962). Mode of action of pineal nerve fibers in frogs. *J. Neurophysiol.* **25**, 405–429.
- Doty, E. and Meissl, H. (1982). The pineal and parietal organs of lower vertebrates. *Experientia* **38**, 996–1000.
- Doty, E. and Morita, Y. (1964). Purkinje-verschiebung, absolute Schwelle und adaptives Verhalten einzelner Elemente der intrakraniellen Anuren-Epiphyse. *Vision Res.* **4**, 413–421.
- Doty, E. and Scherer, E. (1968). Photoc responses from the parietal eye of the lizard *Lacerta sicula campestris* (De Betta). *Vision Res.* **8**, 61–72.
- Drivenes, O., Soviknes, A. M., Ebbesson, L. O. E., Fjose, A., Seo, H.-C. and Helvik, J. V. (2003). Isolation and characterization of two teleost melanopsin genes and their differential expression within the inner retina and brain. *J. Comp. Neurol.* **456**, 84–93.
- Forsell, J., Ekstrom, P., Flamarique, I. N. and Holmqvist, B. (2001). Expression of pineal ultraviolet- and green-like opsins in the pineal organ and retina of teleosts. *J. Exp. Biol.* **204**, 2517–2525.
- Forsell, J., Holmqvist, B. and Ekström, P. (2002). Molecular identification and developmental expression of UV and green opsin mRNAs in the pineal organ of the Atlantic halibut. *Dev. Brain Res.* **136**, 51–62.
- Fujii, R. (1969). Chromatophores and pigments. In *Fish Physiology*, Vol. 3 (ed. W. S. Hoar and D. J. Randall), pp. 307–353. New York: Academic Press.
- Fujii, R. (1993). Cytophysiology of fish chromatophores. *Int. Rev. Cytol.* **143**, 191–255.
- Fujii, R., Wakatabi, H. and Oshima, N. (1991). Inositol 1,4,5-trisphosphate signals the motile response of fish chromatophores. I. Aggregation of pigment in the tilapia melanophore. *J. Exp. Zool.* **259**, 9–17.
- Govardovskii, V. I., Fyhrquist, N., Reuter, T., Kuzmin, D. G. and Donner, K. (2000). In search of the visual pigment template. *Vis. Neurosci.* **17**, 509–528.
- Halstenberg, S., Lindgren, K. M., Samagh, S. P. S., Nadal-Vicens, M., Balt, S. and Fernald, R. D. (2005). Diurnal rhythm of cone opsin expression in the teleost fish *Haplochromis burtoni*. *Vis. Neurosci.* **22**, 135–141.
- Hartwig, H.-G. and Baumann, C. (1974). Evidence for photosensitive pigments in the pineal complex of the frog. *Vision Res.* **14**, 597–598.
- Hawkes, J. W. (1974). The structure of fish skin. II. The chromatophore unit. *Cell Tissue Res.* **149**, 159–172.
- Hawryshyn, C. W. (1991). Light-adaptation properties of the ultraviolet-sensitive cone mechanism in comparison to the other receptor mechanisms of goldfish. *Vis. Neurosci.* **6**, 293–301.
- Hawryshyn, C. W. and Beauchamp, R. (1985). Ultraviolet photosensitivity in goldfish: an independent UV retinal mechanism. *Vision Res.* **25**, 11–20.
- Hawryshyn, C. W., Ramsden, S. D., Betke, K. M. and Sabbah, S. (2010). Spectral and polarization sensitivity of juvenile Atlantic salmon (*Salmo salar*): phylogenetic considerations. *J. Exp. Biol.* **213**, 3187–3197.
- Hayashi, H., Sugimoto, M., Oshima, N. and Fujii, R. (1993). Circadian motile activity of erythrophores in the red abdominal skin of tetra fishes and its possible significance in chromatic adaptation. *Pigment Cell Res.* **6**, 29–36.
- Hornsby, M. A. W., Sabbah, S., Robertson, R. M. and Hawryshyn, C. W. (2013). Modulation of environmental light alters reception and production of visual signals in Nile tilapia. *J. Exp. Biol.* **216**, 3110–3122.

- Im, L. H. J., Isoldi, M. C., Scarparo, A. C., Visconti, M. A. and de Lauro Castrucci, A. M. (2007). Rhythmic expression, light entrainment and alpha-MSH modulation of rhodopsin mRNA in a teleost pigment cell line. *Comp. Biochem. Physiol. A Mol. Integr. Physiol.* **147**, 691-696.
- Johnson, A. M., Stanis, S. and Fuller, R. C. (2013). Diurnal lighting patterns and habitat alter opsin expression and colour preferences in a killifish. *Proc. R. Soc. B* **280**, 1-8.
- Kasai, A. and Oshima, N. (2006). Light-sensitive motile iridophores and visual pigments in the neon tetra, *Paracheirodon innesi*. *Zool. Sci.* **23**, 815-819.
- Kojima, D., Mano, H. and Fukada, Y. (2000). Vertebrate ancient-long opsin: a green-sensitive photoreceptive molecule present in zebrafish deep brain and retinal horizontal cells. *J. Neurosci.* **20**, 2845-2851.
- Korenbrot, J. I. and Fernald, R. D. (1989). Circadian rhythm and light regulate opsin mRNA in rod photoreceptors. *Nature* **337**, 454-457.
- Koyanagi, M., Kawano, E., Kinugawa, Y., Oishi, T., Shichida, Y., Tamotsu, S. and Terakita, A. (2004). Bistable UV pigment in the lamprey pineal. *Proc. Natl. Acad. Sci. USA* **101**, 6687-6691.
- Leow, E. R. (1995). Determinants of visual pigment spectral location and photoreceptor cell spectral sensitivity. In *Neurobiology and Clinical Aspects of the Outer Retina* (ed. M. B. A. Djamgoz, S. N. Archer and S. Vallergera), pp. 57-77. London: Chapman & Hall.
- Lisney, T. J., Studd, E. and Hawryshyn, C. W. (2010). Electrophysiological assessment of spectral sensitivity in adult Nile tilapia *Oreochromis niloticus*: evidence for violet sensitivity. *J. Exp. Biol.* **213**, 1453-1463.
- Luby-PHELPS, K. and Porter, K. R. (1982). The control of pigment migration in isolated erythrophores of *Holocentrus ascensionis* (Osbeck). II. The role of calcium. *Cell* **29**, 441-450.
- Lucas, R. J., Hattar, S., Takao, M., Berson, D. M., Foster, R. G. and Yau, K.-W. (2003). Diminished pupillary light reflex at high irradiances in melanopsin-knockout mice. *Science* **299**, 245-247.
- Mano, H., Kojima, D. and Fukada, Y. (1999). Exo-rhodopsin: a novel rhodopsin expressed in the zebrafish pineal gland. *Mol. Brain Res.* **73**, 110-118.
- Masada, M., Matsumoto, J. and Akino, M. (1990). Biosynthetic pathways of pteridines and their association with phenotypic expression in vitro in normal and neoplastic pigment cells from goldfish. *Pigment Cell Res.* **3**, 61-70.
- Masagaki, A. and Fujii, R. (1999). Differential actions of melatonin on melanophores of the threeline pencilfish, *Nannostomus trifasciatus*. *Zool. Sci.* **16**, 35-42.
- Mähger, L. M., Land, M. F., Siebeck, U. E. and Marshall, N. J. (2003). Rapid colour changes in multilayer reflecting stripes in the paradise whiptail, *Pentapodus paradiseus*. *J. Exp. Biol.* **206**, 3607-3613.
- Meissl, H. and Ekström, P. (1988). Photoreceptor responses to light in the isolated pineal organ of the trout, *Salmo gairdneri*. *Neuroscience* **25**, 1071-1076.
- Meissl, H. and Ueck, M. (1980). Extraocular photoreception of the pineal gland of the aquatic turtle *Pseudemys scripta elegans*. *J. Comp. Physiol. A Neuroethol. Sens. Neural. Behav. Physiol.* **140**, 173-179.
- Meissl, H. and Yanez, J. (1994). Pineal photosensitivity: a comparison with retinal photoreception. *Acta Neurobiol. Exp. (Warsaw)* **54**, 19-29.
- Miyashita, Y., Moriya, T., Yamada, K., Kubota, T., Shirakawa, S., Fujii, N. and Asami, K. (2001). The photoreceptor molecules in *Xenopus* tadpole tail fin, in which melanophores exist. *Zool. Sci.* **18**, 671-674.
- Moriya, T., Miyashita, Y., Arai, J.-I., Kusunoki, S., Abe, M. and Asami, K. (1996). Light-sensitive response in melanophores of *Xenopus laevis*: I. Spectral characteristics of melanophore response in isolated tail fin of *Xenopus* tadpole. *J. Exp. Zool.* **276**, 11-18.
- Nakane, Y., Ikegami, K., Ono, H., Yamamoto, N., Yoshida, S., Hirunagi, K., Ebihara, S., Kubo, Y. and Yoshimura, T. (2010). A mammalian neural tissue opsin (Opsin 5) is a deep brain photoreceptor in birds. *Proc. Natl. Acad. Sci. USA* **107**, 15264-15268.
- Naora, H., Takabatake, I. and Iga, T. (1988). Spectral sensitivity of melanophores of a freshwater teleost, *Zacco temminckii*. *Comp. Biochem. Physiol. A* **90**, 147-149.
- Nilsson Sköld, H., Aspöngren, S. and Wallin, M. (2013). Rapid color change in fish and amphibians: function, regulation, and emerging applications. *Pigment Cell Melanoma Res.* **26**, 29-38.
- Oshima, N., Makino, M., Iwamuro, S. and Bern, H. A. (1996). Pigment dispersion by prolactin in cultured xanthophores and erythrophores of some fish species. *J. Exp. Zool.* **275**, 45-52.
- Oshima, N., Nakata, E., Ohta, M. and Kamagata, S. (1998). Light-induced pigment aggregation in xanthophores of the medaka, *Oryzias latipes*. *Pigment Cell Res.* **11**, 362-367.
- Panda, S., Sato, T. K., Castrucci, A. M., Rollag, M. D., DeGrip, W. J., Hogenesch, J. B., Provencio, I. and Kay, S. A. (2002). Melanopsin (Opn4) requirement for normal light-induced circadian phase shifting. *Science* **298**, 2213-2216.
- Philp, A. R., Garcia-Fernandez, J. M., Soni, B. G., Lucas, R. J., Bellingham, J. and Foster, R. G. (2000). Vertebrate ancient (VA) opsin and extraretinal photoreception in the Atlantic salmon (*Salmo salar*). *J. Exp. Biol.* **203**, 1925-1936.
- Provencio, I., Jiang, G., De Grip, W. J., Hayes, W. P. and Rollag, M. D. (1998). Melanopsin: an opsin in melanophores, brain, and eye. *Proc. Natl. Acad. Sci. USA* **95**, 340-345.
- Sabbah, S., Laria, R. L., Gray, S. M. and Hawryshyn, C. W. (2010). Functional diversity in the color vision of cichlid fishes. *BMC Biol.* **8**, 133.
- Sabbah, S., Hui, J., Hauser, F. E., Nelson, W. A. and Hawryshyn, C. W. (2012). Ontogeny in the visual system of Nile tilapia. *J. Exp. Biol.* **215**, 2684-2695.
- Sato, M., Ishikura, R. and Oshima, N. (2004). Direct effects of visible and UVA light on pigment migration in erythrophores of Nile tilapia. *Pigment Cell Res.* **17**, 519-524.
- Shand, J. and Foster, R. G. (1999). The extraretinal photoreceptors of non-mammalian vertebrates. In *Adaptive Mechanisms in the Ecology of Vision* (ed. S. N. Archer, M. B. A. Djamgoz, E. R. Leow, J. C. Partridge and S. Vallergera), pp. 197-222. Dordrecht, The Netherlands: Kluwer Academic Publishers.
- Solessio, E. and Engbretson, G. A. (1993). Antagonistic chromatic mechanisms in photoreceptors of the parietal eye of lizards. *Nature* **364**, 442-445.
- Spady, T. C., Parry, J. W. L., Robinson, P. R., Hunt, D. M., Bowmaker, J. K. and Carleton, K. L. (2006). Evolution of the cichlid visual palette through ontogenetic subfunctionalization of the opsin gene arrays. *Mol. Biol. Evol.* **23**, 1538-1547.
- Uchida, K. and Morita, Y. (1990). Intracellular responses from UV-sensitive cells in the photosensory pineal organ. *Brain Res.* **534**, 237-242.
- Uchida, K. and Morita, Y. (1994). Spectral sensitivity and mechanism of interaction between inhibitory and excitatory responses of photosensory pineal neurons. *Pflugers Arch.* **427**, 373-377.
- Vigh, B., Manzano, M. J., Zádori, A., Frank, C. L., Lukáts, A., Röhlich, P., Szél, A. and Dávid, C. (2002). Nonvisual photoreceptors of the deep brain, pineal organs and retina. *Histol. Histopathol.* **17**, 555-590.
- Wada, S., Kawano-Yamashita, E., Koyanagi, M. and Terakita, A. (2012). Expression of UV-sensitive parainopsin in the iguana parietal eyes and its implication in UV-sensitivity in vertebrate pineal-related organs. *PLoS ONE* **7**, e39003.
- Yamashita, T., Ohuchi, H., Tomonari, S., Ileda, K., Sakai, K. and Shichida, Y. (2010). Opn5 is a UV-sensitive bistable pigment that couples with Gi subtype of G protein. *Proc. Natl. Acad. Sci. USA* **107**, 22084-22089.